Conformational entropy of intrinsically disordered proteins bars intruders from biomolecular condensates

Vladimir Grigorev,[1] Ned S. Wingreen,[2,3,*] and Yaojun Zhang[1,4,*]

[1] *Department of Physics and Astronomy, Johns Hopkins University, Baltimore, MD, USA*
[2] *Department of Molecular Biology, Princeton University, Princeton, NJ, USA*
[3] *Lewis-Sigler Institute for Integrative Genomics, Princeton University, Princeton, NJ, USA*
[4] *Department of Biophysics, Johns Hopkins University, Baltimore, MD, USA*

(Dated: March 3, 2023)

It has recently been discovered that eukaryotic cells are host to a multiplicity of biomolecular condensates. These condensates typically contain protein components with intrinsically disordered regions (IDRs). While IDRs have been proposed and demonstrated to play many roles in the literature, we suggest here an additional crucial role of IDRs, which is to exclude unwanted "intruders" from condensates. This exclusion effect arises from the large conformational entropy of IDRs, i.e., there is a large free-energy cost to occupying volume that would otherwise be available to the IDRs. We find that at realistic IDR densities, particles as small as the size of an average protein (4 nm in diameter) can be more than 98% excluded from condensates. Application of the developed size-exclusion theory to biological condensates suggests that condensate IDRs may play a generic exclusionary role across organisms and types of condensates.

I. INTRODUCTION

Many of the macromolecular components of cells – proteins, RNAs, and DNA – are now known to be spatially partitioned into distinct phase-separated condensates [1, 2]. However, what leads particular components to be included in or excluded from each type of condensate remains poorly understood. The components of biomolecular condensates are generally divided into two categories, scaffolds and clients [3]: The small number of components responsible for condensate formation are referred to as scaffolds. Deletion or depletion of these molecules can abolish phase separation. Other molecules that are located within the structure but do not drive phase separation are referred to as clients. Clients are typically recruited into a condensate through binding of complementary motifs to scaffolds. It is however not clear how condensates keep out irrelevant molecules. Specifically, for an intracellular condensate immersed in a cellular milieu, it faces thousands of different types of molecules. How does it exclude irrelevant molecules to maintain a specific set of desired components?

A notable feature of many of the scaffold proteins that drive phase separation is that they contain large intrinsically disordered regions (IDRs). These IDRs are believed to play many roles, including modulating condensate stability, modifying condensate physical properties such as density and internal diffusivity, and providing binding sites for clients [4]. We propose here an additional important role of IDRs, namely to exclude large undesired macromolecules from condensates (Fig. 1). Indeed, it has been observed that condensates follow a generic size-exclusion principle, i.e., condensates exclude large molecules. For example, while 10 kDa dextran molecules strongly partition into LAF-1 and NPM1 droplets *in vitro* and *in vivo*, 70 and 155 kDa dextran molecules are mostly excluded [5]. Similarly, perinuclear P granules in *Caenorhabditis elegans* exclude molecules larger than $\sim$ 70 kDa [6]. Another example is the algal pyrenoid which excludes proteins larger than $\sim$ 80 kDa [7]. In addition, a recent study [8] reporting the discovery of repressive condensates in *Ciona* embryos suggested that these condensates might function by excluding the larger machinery of transcription, including RNA polymerases ($\sim$ 500 kDa), Mediator complexes ($\sim$ 1 MDa), and transcriptionally activating histone modifiers and nucleosome remodelers ($\sim 1-3$ MDa). All these condensates contain scaffold molecules with large IDRs.

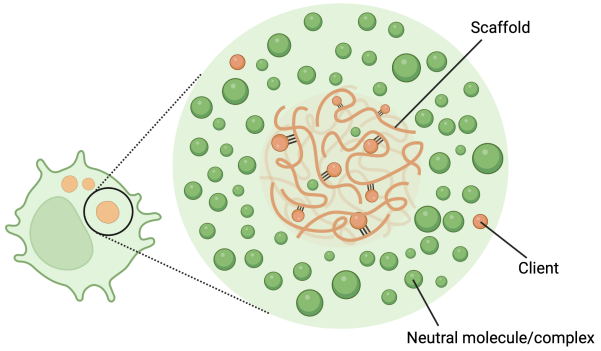

FIG. 1. Schematic of particle exclusion from a biomolecular condensate.

Due to the polymer nature of IDRs, if the scaffolds span the entire condensate and form a stable gel network with fixed mesh size(s) as was proposed in [9], then it is obvious that any molecule larger than the size of the mesh will be excluded from the condensate. We would thus expect a hard size cutoff for clients found in the

* Email: wingreen@princeton.edu; yaojunz@jhu.edu

condensate. However, biomolecular condensates are network fluids, i.e., the network is dynamic and local interactions form and dissolve quickly. It is then unclear how such a liquid condensate could exclude molecules, as large molecules could always enter the condensate though large transient holes. We show below that the conformational entropy of IDRs is the key factor leading to the exclusion of large particles from condensates. Compared to folded domains, IDRs have much higher conformational entropy, and this implies that removing any of the volume accessible to IDRs has a high free-energy cost. In effect, IDRs create a "pressure" inside of condensates, which can exclude sufficiently large molecules.

II. RESULTS

A. Entropy of IDRs excludes particles from a model condensate.

To demonstrate the ability of polymer conformational entropy to exclude neutral particles from biomolecular condensates, we performed coarse-grained molecular-dynamics simulations of sticker-spacer polymers [10], Fig. 2 and see Methods. Briefly, we model polymers as flexible linear chains of spherical beads connected by stretchable springs. Sticker beads of two types - A (blue) and B (red) - can form one-to-one heterotypic A:B bonds via a short-ranged attractive interaction. Spacer beads (white), sticker beads of the same type, and neutral particles (green) interact with each other via short-ranged repulsive interactions. The attraction between A and B stickers drives polymer phase separation. Simulations are performed using the LAMMPS Molecular Dynamics Simulator [11].

We first simulated a condensate in which the spacers are single lumped spherical beads. In this case, the spacers have no conformational entropy *per se* even though they do exclude volume. As shown in Fig. 2a,e, the resulting sticker-spacer condensate partially excludes neutral particles, but the concentration of particles is only reduced by $\sim$ 2-fold compared to the surrounding region. By contrast, as shown in Fig. 2b,f, if we replace the single spacer beads by chains of smaller beads of the same total volume, the neutral particle concentration in the dense phase is now reduced $\sim$ 15-fold. The only essential difference between the two cases is that the spacers in the latter case have conformational entropy. This simple model makes it clear that explicit spacers in the form of IDRs can provide strong exclusion (Fig. 2, *right*), whereas exclusion is nearly absent if the same spacer volume is collapsed into folded domains (Fig. 2, *left*).

B. IDRs impose a free-energy barrier to "intruder" particles.

The exclusion of neutral particles by explicit IDRs observed in Fig. 2 reflects the free-energy cost of adding a neutral particle to the condensate. In effect, the presence of the neutral particle reduces the possible conformations of the IDRs, and this reduction of IDR entropy implies an increase of the system's free energy. To quantify this free-energy barrier (Fig. 3), we inserted spherical test particles of radius R at random locations in the condensates shown in Fig. 2a,b. For each insertion, we calculated the energy $U(R)$ due to the repulsive, steric interactions between the test particle and the local contents of the condensate (see Methods). The free-energy cost of the insertion is given by the average of the resulting Boltzmann factors:

$$\Delta F(R) = -k_{\mathrm{B}}T \ln \left\langle e^{-\frac{U(R)}{k_{\mathrm{B}}T}} \right\rangle, \tag{1}$$

where k_{B} is the Boltzmann constant and T is the temperature of the system. As shown in Fig. 3a, over a large range of test particle radii, the free-energy barrier is substantially higher for the condensate with multiple small spacer beads (Fig. 2b) than for the condensate with a single lumped spacer bead (Fig. 2a). To understand this difference, we consider the probability that a randomly inserted test particle will overlap with a spacer bead in either case. Even though the two types of spacer occupy the same total volume, the probability of an overlap is much larger for the small beads. This is because the test particle only has to come within the combined radius, $R_{\text{test particle}} + R_{\text{spacer bead}}$, to create a steric overlap. For small spacer beads the region of overlap becomes a tube of radius $R_{\text{test particle}}$ independent of the radius of the spacer bead. Thus, increasing the number of spacer beads while keeping their total volume fixed increases the length of the tube of "exclusion" without decreasing its radius. This is why the free-energy barrier for test particles is generally higher for the case of small linker beads.

The free energy in Eq. (1) allows a prediction of the partition coefficient for particles between a condensate and the surrounding dilute phase. Specifically, the partition coefficient is predicted to be

$$P(R) = e^{-\frac{\Delta F(R)}{k_{\mathrm{B}}T}}. \tag{2}$$

We note that this prediction applies rigorously to the case where the condensate is confined to a fixed volume. In the simulation in Fig. 2a, the volume occupied by the condensate adjusts due to the presence of particles both inside the condensate, which tend to make the condensate swell, and outside the condensate, whose "pressure" tends to make the condensate contract. However, the net change in condensate volume is very small, $\sim$ 3%, and the measured partition coefficient in Fig. 2e,f ("+" symbol in Fig. 3b) is indeed very close to that obtained using the bead-insertion method (Fig. 3b).

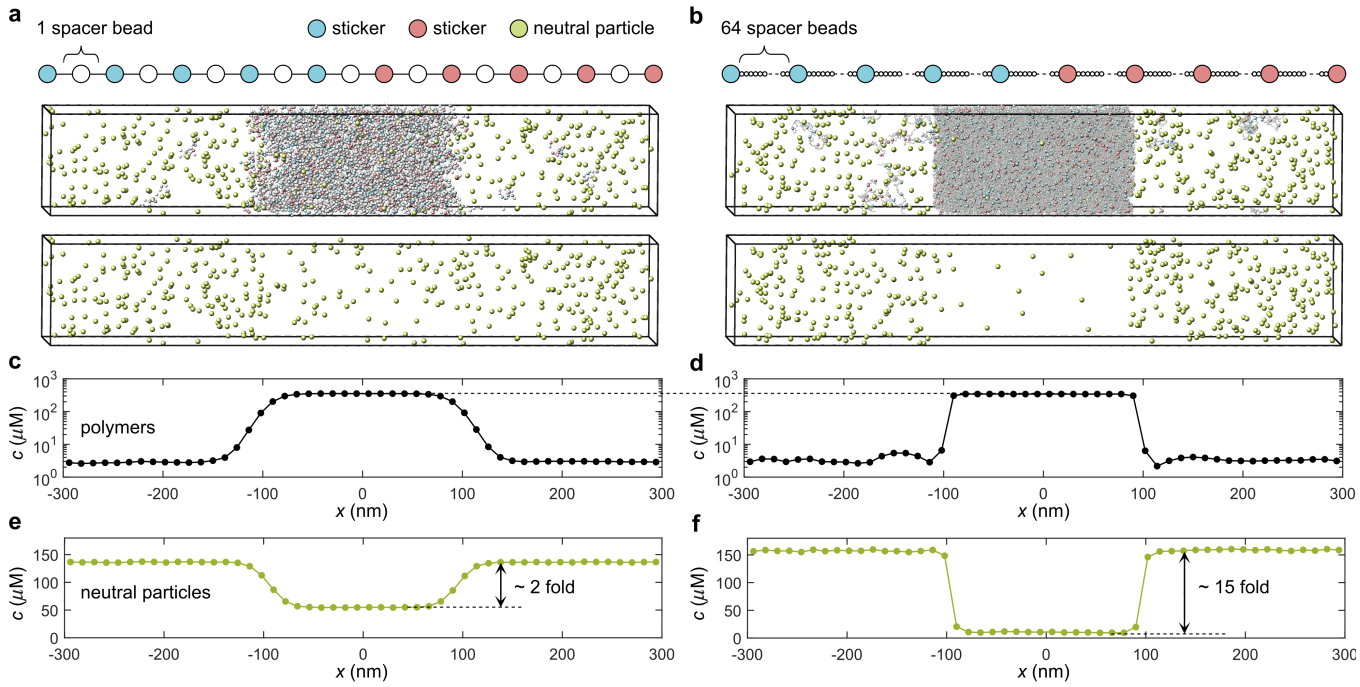

FIG. 2. Intrinsically disordered spacer regions strongly exclude neutral particles from a simulated biomolecular condensate. **a**, Snapshot of a coarse-grained molecular-dynamics simulation of 400 sticker-spacer polymers and 400 neutral particles of diameter 5 nm (green), where each polymer is modeled as a linear chain of spherical particles, 5 sticker A (red), 5 sticker B (blue), and 9 spacer (white) all of diameter 3 nm, connected by stretchable bonds. The system phase separates into a dense phase (middle region) and a dilute phase (two sides) in a 600 nm × 100 nm × 100 nm box with periodic boundary conditions. **b**, Similar to **a**, but with spacers composed of 64 small beads each of diameter 0.75 nm, whose total volume equals that of one spacer bead in **a**. To make a fair comparison, we imposed hard wall boundaries to confine the dense phase to make the total volume occupied by polymers the same as in **a** (both at 4.8%). Specifically, walls that are impenetrable to the polymers were imposed at $x = \pm 100$ nm. **c**, **d**, Polymer concentration profile of systems in **a**, **b** averaged over time and over 10 simulation replicates, with the center of the dense phase fixed at $x = 0$. **e**, **f**, Neutral particle concentration profile of systems in **a**, **b**, respectively. All simulations performed and simulation snapshots taken in LAMMPS [11], see Methods for simulation details.

The simulated condensate in Fig.2b contains stickers and spacers, where the stickers resemble the structured domains and the spacers resemble the IDRs of proteins. To disentangle the contributions from stickers and spacers to the exclusion of neutral particles, we simulated a "spacers-only" condensate. Briefly, we first measured the volume fraction of spacers in the dense phase of the condensate in Fig. 2b (2.8%). We then removed all the sticker beads in the model polymer and reconnected the spacers to form a spacers-only polymer. Such polymers are then confined in a simulation box of the proper size to yield 2.8% volume fraction. The free-energy barriers and partition coefficients of spherical particles for the spacers-only condensate are obtained following the same particle insertion procedure. Comparing to the sticker-spacer condensate (Fig. 3, filled red circle), we find that the spacer-only condensate excludes particles to a comparable degree (Fig. 3, open red circle). Therefore, we conclude that the conformational entropy of IDRs is the key factor leading to the exclusion of large particles from the condensates.

C. Polymer theory for size exclusion

Above, we derived the free-energy barrier in terms of the energetic cost of inserting a test particle, Eq. (1). One can equally derive the free-energy barrier via the reduction of conformational entropy of the IDRs. In fact, maximizing the conformational entropy of polymers is the origin of depletion forces between colloidal particles suspended in a polymer solution [12, 13]. There are, however, only a limited number of studies aimed at quantifying the free-energy cost of inserting a particle into a polymer solution [14–17]. It is expected that for a semi-dilute solution of flexible chains in a good solvent, the free-energy cost of inserting a non-absorbing spherical particle obeys the following scaling relationship [14]

$$\Delta F(R) = k_{\mathrm{B}}T \begin{cases} a_1 \left(\frac{R}{\xi}\right)^{3-\frac{1}{\nu}}, & R \ll \xi; \\ a_2 \left(\frac{R}{\xi}\right)^2 + a_3 \left(\frac{R}{\xi}\right)^3, & R \gg \xi, \end{cases} \tag{3}$$

where R is the particle radius, $\nu = 0.588$ is the Flory exponent, ξ is the polymer correlation length (or "blob size"), and a_1, a_2, a_3 are constant prefactors.

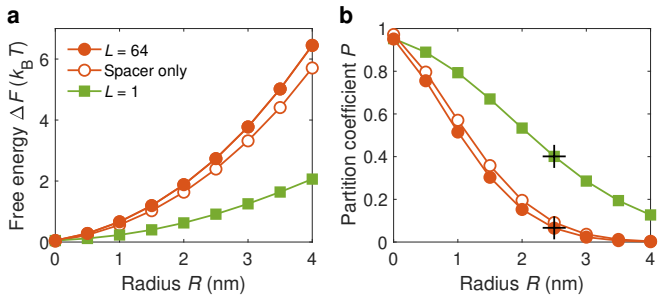

FIG. 3. Intrinsically disordered spacer regions increase free-energy cost of inserting neutral particles into simulated biomolecular condensates. **a**, Free-energy cost ΔF of inserting neutral test particles as a function of particle radius R, using Eq. (1). Particles are inserted into the (frozen) dense phase of the condensates shown in Fig. 2a (spacer length $L = 1$, green) and Fig. 2b (spacer length $L = 64$, red filled), and into a homogeneous "spacers-only" polymer solution with a volume fraction matched to that of the spacers in the Fig. 2b condensate (spacer only, red open). The spacers-only polymer solution contains 27 flexible self-avoiding bead-spring polymers each with 576 monomers of diameter 0.75 nm in a simulation box of side length 50.5 nm with periodic boundary conditions, yielding a volume fraction of 2.8%. **b**, The corresponding partition coefficient P of particles predicted by Eq. (2) using ΔF obtained in **a**. The black "+" are data points obtained from the simulation results in Fig. 2e,f, i.e., the concentration ratio of the 5 nm diameter particles in the dense and dilute phases. See Methods for details.

.

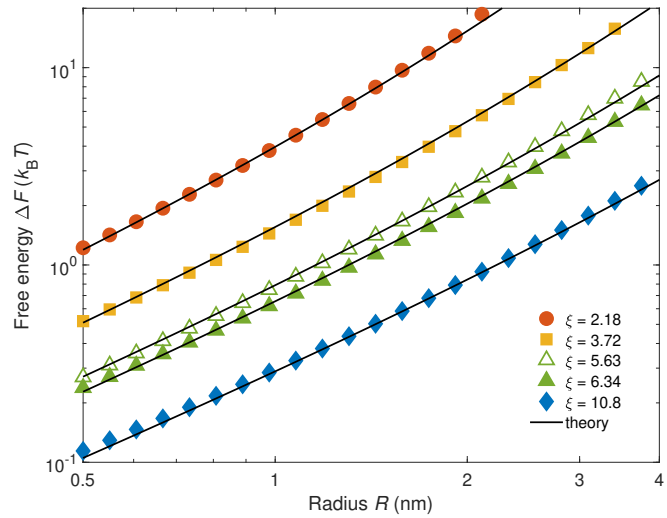

FIG. 4. Simulated free-energy costs of inserting spherical particles into homogeneous polymer solutions are captured by the theoretical expression in Eq. (4). All polymer systems contain 27 self-avoiding bead-spring polymers each with 400 monomers of diameter 0.38 nm (average size of an amino acid residue) in simulation boxes of varying sizes with periodic boundary conditions. Red, yellow, green, and blue filled symbols are for fully flexible polymers in boxes of side length 17.6, 22.2, 28.0, and 35.3 nm. Green open symbols are for polymers with a higher persistence length in a box of length 28.0 nm. The correlation length ξ for each system is calculated by first measuring the osmotic pressure Π in the polymer solution and then using the inverse of Eq. (5), i.e., $\xi = [k_{\rm B}T/(3\nu-1)/\Pi)]^{1/3}$. Black curves are from a global fit of the theoretical expression in Eq. (4) to results from all simulations. The prefactor 4.7 in Eq. (4) is a parameter from the fit.

To obtain a more precise expression for the free-energy of insertion, we simulated spacers-only polymers at different volume fractions and with different persistence lengths to yield a wide range of correlation lengths, and then obtained the free-energy cost of insertion (Fig. 4) using Eq. (1). Based on these simulation results and the scaling relationship in Eq. (3), we propose that

$$\Delta F(R) = 4.7 k_{\rm B}T \left(\frac{R}{\xi}\right)^{3-\frac{1}{\nu}} + \Pi\left(2\pi R^2\xi + \frac{4\pi}{3}R^3\right), \quad (4)$$

where Π is the osmotic pressure from the polymers, which is directly accessible from simulations, and

$$\Pi = \frac{k_{\rm B}T}{(3\nu-1)\xi^3}. \quad (5)$$

The first term in Eq. (4) is the free-energy cost of inserting a small particle into a blob, i.e., the first term in Eq. (3). The prefactor $a_1 = 4.7$ was obtained from a global fit of simulation results at different ξ, Fig. 4 (see Methods for details). The second and third terms come from the free-energy cost of having the polymer blobs avoid a large particle as a whole: the free-energy cost is $\Pi\Delta V$ with the excluded volume $\Delta V = 4\pi(R+\xi/2)^3/3 \approx 2\pi R^2\xi + 4\pi R^3/3$. One can equally view the free-energy barrier as the amount of work needed to grow a particle to radius R in a polymer solution, i.e.,

$$\Delta F(R) = \int_0^R 4\pi r^2 p(r)dr, \quad (6)$$

where $p(r)$ is the pressure on a particle of radius r from the polymers. In the large R limit, $p(R)$ approaches the osmotic pressure Π, Eq. (6) is then $\Delta F(R) = 4\pi R^3\Pi/3$ which is consistent with the third term on the right of Eq. (4).

If particles are free to partition away from the region of polymers, then based on Eqs. (2), (4), and (5), a particle of diameter ξ, i.e. the size of a blob, has a free energy of insertion $\Delta F = 4.6k_{\rm B}T$ and a partition coefficient $P = 0.01$, which means that there is a 100-fold reduction in its concentration in the polymer rich region. In fact, the partition coefficient of a particle is only determined by the ratio of its size and the correlation length of the polymer system. We note that in the simulations in Fig. 4, we obtained ξ for each system by measuring the osmotic pressure and then inverting the relationship in Eq. (5). However, osmotic pressure is not always accessible and Eq. (5) does not strictly apply in the presence of stickers. Alternatively, the correlation length of a semi-

dilute polymer solution scales as $\xi \sim \phi^{-\nu/(3\nu-1)}d$ [18], where ϕ is the volume fraction of polymers in solution and d is the diameter of a monomer. Based on our simulation results, we found that

$$\xi = 0.63\phi^{-\frac{\nu}{3\nu-1}}d \tag{7}$$

for fully flexible self-avoiding chains, whereas ξ is less than the value predicted by Eq. (7) for chains with a longer persistence length.

D. Application of the size-exclusion theory to biological condensates

How well does the size-exclusion theory apply to biological condensates? Ref. [5] studied the partitioning of various dextrans into LAF-1 condensates. The measured concentration of LAF-1 protein in the *in vitro* condensates was $\sim$ 2.6 mM [19]. Each LAF-1 has about 250 amino acids in the disordered regions [20]. Assuming each amino-acid residue is a sphere of diameter 0.38 nm, the volume fraction of IDRs is then 1.1%. The IDR correlation length in the LAF-1 condensates according to Eq. (7) is then $\xi = 7.6$ nm. The hydrodynamic radii of the 10 kDa, 70 kDa, and 155 kDa dextran probes are 1.9 nm, 6.5 nm, and 8.9 nm [21]. The free energies of insertion for these dextrans are predicted to be 1.4, 13, and 26 $k_{\mathrm{B}}T$ from Eq. (4). Therefore, we expect the 10-kDa dextran to enter the LAF-1 condensate almost freely, whereas the 70-kDa and 155-kDa dextrans should be strongly excluded. This is consistent with the observations in [5].

More generally, the scaffold concentration of biological condensates typically ranges from 80 to 500 g/L with a mean concentration $\sim$ 300 g/L [22]. If we assume each scaffold molecule has half of its amino-acid residues in the IDRs, and take the mass of an amino acid to be 110 g/mole and its diameter to be 0.38 nm, then an "average" condensate has a volume fraction of IDRs 2.4%, which corresponds to a correlation length 4.3 nm. This suggests that proteins as small as 4 nm in diameter ($\sim$ 20 kDa) will already face a free-energy barrier of $4\,k_{\mathrm{B}}T$ to enter the condensate, yielding a partition coefficient 0.02. It is therefore likely that exclusion occurs universally to the majority of proteins in the proteome, i.e., as long as there is no significant binding affinity between a protein and condensate scaffolds (or clients), the protein is generally excluded. Condensates can then achieve component specificity by recruiting only the ones that bind strongly to condensate components.

III. DISCUSSION

We presented simulations and theory that support a possible role for protein IDRs in excluding "unwanted" macromolecules from intracellular condensates. In a nutshell, IDRs and other flexible polymers enjoy high conformational entropy – thus any restriction of the volume available to these polymers reduces this entropy and so has a free-energy cost. In particular, adding a macromolecule or other particle to a condensate reduces the volume available to the IDRs, which implies the existence of a free-energy barrier to "intruders". The magnitude of this barrier depends on the size (and to a lesser extent the shape) of the intruding particle as well as on the properties of the IDRs. Roughly speaking, the IDRs impose a pressure on the particle, and the free-energy barrier reflects the pressure-volume work required to insert the particle into the condensate (Fig. 4). Thus, in general, larger particles experience higher barriers to entry.

It is worth noting that the entropic pressure imposed by IDRs does not directly depend on the fraction of condensate volume the IDRs occupy. A useful analogy is the pressure of an ideal gas, which is proportional to the number density of particles, independent of the volume of each particle. Rather, the ideal gas pressure is due to the translational entropy of the center of mass of each gas particle, independent of its volume. The pressure of IDRs is a restricted form of this gas pressure in which the IDR residues are like gas particles that are restricted in their motion by being connected to their neighbors. Thus the entropic pressure of IDRs is always less than it would be if the IDR residues were disconnected (though in this case, the residues would be free to escape the condensate). The connectivity of IDRs reduces their pressure to that of a "gas of blobs" [Eq. (5), note that $1/\xi^3$ in the equation is essentially the number density of blobs], where each blob is a section of polymer chain that behaves as a self-avoiding random walk.

Particles may also be excluded from a condensate because of changes to the chemical environment within the condensate. Indeed, it has been recently shown that small molecules (metabolites and drugs $\sim$ 1 nm) may prefer to be in or out of specific condensates, depending on each molecule's chemical character [23]. For these small molecules, the free-energy difference in and out of condensates is presumably mostly due to the interactions of the molecules with the chemical environment inside the condensate, not to the entropic exclusion from IDRs, as the entropic barrier is negligible for these small molecules ($< 1k_{\mathrm{B}}T$). For larger molecules, such as proteins or RNAs, both the entropic exclusion and interactions with the condensate components and/or chemical environment will contribute to the free-energy barrier – in the case where the interactions are strong and favorable, the free energy may be negative, making the molecule a "client" that preferentially partitions into the condensate.

Our proposal that IDRs can exclude unwanted particles from biomolecular condensates is consistent with the many other roles played by IDRs, from holding condensates together, to providing binding sites for clients, to fine-tuning condensate properties. Indeed, one of the proposed roles of IDRs is to reduce condensate density via IDR-IDR self-avoidance. This self-avoidance reflects

the same tendency of flexible polymers to maximize their conformational entropy that we explored here as the driving force for exclusion of irrelevant molecules. Going forward, we hope that experimental approaches will clarify the extent to which real IDRs exclude particles from both natural and synthetic condensates.

ACKNOWLEDGMENTS

VG and YZ were supported by a startup fund at Johns Hopkins University. NSW was supported by the National Science Foundation, through the Center for the Physics of Biological Function (PHY-1734030), NIH Grant R01 GM140032, and Princeton Biomolecular Condensate Program.

[1] S. F. Banani, H. O. Lee, A. A. Hyman, and M. K. Rosen, Biomolecular condensates: Organizers of cellular biochemistry, Nat. Rev. Mol. Cell Biol. **18**, 285 (2017).

[2] Y. Shin and C. P. Brangwynne, Liquid phase condensation in cell physiology and disease, Science **357**, 4382 (2017).

[3] J. A. Ditlev, L. B. Case, and M. K. Rosen, Who's in and who's out–compositional control of biomolecular condensates, J. Mol. Biol. **430**, 4666 (2018).

[4] J. D. Forman-Kay and T. Mittag, From sequence and forces to structure, function, and evolution of intrinsically disordered proteins, Structure **21**, 1492 (2013).

[5] M.-T. Wei, S. Elbaum-Garfinkle, A. S. Holehouse, C. C.-H. Chen, M. Feric, C. B. Arnold, R. D. Priestley, R. V. Pappu, and C. P. Brangwynne, Phase behaviour of disordered proteins underlying low density and high permeability of liquid organelles, Nature chemistry **9**, 1118 (2017).

[6] D. L. Updike, S. J. Hachey, J. Kreher, and S. Strome, P granules extend the nuclear pore complex environment in the c. elegans germ line, Journal of Cell Biology **192**, 939 (2011).

[7] L. C. Mackinder, C. Chen, R. D. Leib, W. Patena, S. R. Blum, M. Rodman, S. Ramundo, C. M. Adams, and M. C. Jonikas, A spatial interactome reveals the protein organization of the algal co2-concentrating mechanism, Cell **171**, 133 (2017).

[8] N. Treen, S. F. Shimobayashi, J. Eeftens, C. P. Brangwynne, and M. Levine, Properties of repression condensates in living ciona embryos, Nature communications **12**, 1561 (2021).

[9] P. L. Paine, L. C. Moore, and S. B. Horowitz, Nuclear envelope permeability, Nature **254**, 109 (1975).

[10] J.-M. Choi, A. S. Holehouse, and R. V. Pappu, Physical principles underlying the complex biology of intracellular phase transitions, Annu. Rev. Biophys. **49** (2020).

[11] LAMMPS Molecular Dynamics Simulator. Available from https://lammps.sandia.gov/.

[12] X.-Z. Cao, H. Merlitz, C.-X. Wu, and J.-U. Sommer, Polymer-induced entropic depletion potential, Physical Review E **84**, 041802 (2011).

[13] D. Meng, S. K. Kumar, S. Cheng, and G. S. Grest, Simulating the miscibility of nanoparticles and polymer melts, Soft Matter **9**, 5417 (2013).

[14] P. G. de Gennes, Suspensions colloidales dans une solution de polymeres, CR Acad. Sc. Paris **288**, 359 (1979).

[15] E. Eisenriegler, A. Hanke, and S. Dietrich, Polymers interacting with spherical and rodlike particles, Physical Review E **54**, 1134 (1996).

[16] A. Hanke, E. Eisenriegler, and S. Dietrich, Polymer depletion effects near mesoscopic particles, Physical Review E **59**, 6853 (1999).

[17] E. Eisenriegler, Small mesoscopic particles in dilute and semidilute solutions of nonadsorbing polymers, The Journal of Chemical Physics **113**, 5091 (2000).

[18] P.-G. De Gennes and P.-G. Gennes, *Scaling concepts in polymer physics* (Cornell university press, 1979).

[19] N. O. Taylor, M.-T. Wei, H. A. Stone, and C. P. Brangwynne, Quantifying dynamics in phase-separated condensates using fluorescence recovery after photobleaching, Biophysical Journal **117**, 1285 (2019).

[20] S. Elbaum-Garfinkle, Y. Kim, K. Szczepaniak, C. C.-H. Chen, C. R. Eckmann, S. Myong, and C. P. Brangwynne, The disordered p granule protein laf-1 drives phase separation into droplets with tunable viscosity and dynamics, Proceedings of the National Academy of Sciences **112**, 7189 (2015).

[21] M. Leduc, D. Guay, R. Leask, and S. Coulombe, Cell permeabilization using a non-thermal plasma, New Journal of Physics **11**, 115021 (2009).

[22] P. M. McCall, K. Kim, A. W. Fritsch, J. Iglesias-Artola, L. Jawerth, J. Wang, M. Ruer, J. Peychl, A. Poznyakovskiy, J. Guck, *et al.*, Quantitative phase microscopy enables precise and efficient determination of biomolecular condensate composition, bioRxiv , 2020 (2020).

[23] S. A. Thody, H. D. Clements, H. Baniasadi, A. S. Lyon, M. S. Sigman, and M. K. Rosen, Small molecule properties define partitioning into biomolecular condensates, bioRxiv , 2022 (2022).